Biomedical Signal Processing and Control 72 (2022) 103322

Contents lists available at ScienceDirect

Biomedical Signal Processing and Control

journal homepage: www.elsevier.com/locate/bspc

Towards classification of patients based on surface EMG data of temporomandibular joint muscles using self-organising maps

Mateusz Troka [a], Wiktoria Wojnicz [b], Katarzyna Szepietowska [a,*], Marek Podlasiński [c], Sebastian Walerzak [c], Konrad Walerzak [c], Izabela Lubowiecka [a]

[a] Faculty of Civil and Environmental Engineering, Gdańsk University of Technology, Poland
[b] Faculty of Mechanical Engineering and Ship Technology, Gdańsk University of Technology, Poland
[c] NZOZ Centrum Leczenia Wad Zgryzu, Warsaw, Poland

ARTICLE INFO

Keywords:
Surface electromyography (sEMG)
Muscle activation
Temporomandibular joint (TMJ)
Jaw motion
Cross-correlation
Self-organising maps (SOM)

ABSTRACT

The study considers the need for an effective method of classification of patients with a temporomandibular joint disorder (TMD). The self-organising map method (SOM) was applied to group patients and used together with the cross-correlation approach to interpret the processed (rectified and smoothed by using root mean square (RMS) algorithm) surface electromyography signal (sEMG) obtained from testing the muscles (two temporal muscles and two masseters) of the temporomandibular joint (TMJ) during selected jaw movements. SOM's Unified distance matrix (U-matrix) maps consist of formed clusters that correspond to similarities in input datasets. The results showed that SOM was able to encode muscular responses and create clusters. Information about the level of similarity between the activity of right, left, ipsilateral, and contralateral pairs of muscles was provided by intra cross-correlation coefficient (CC). A low intra CC value may indicate instability of the TMJ function. Information about the level of similarity between the sEMG signals of the same muscles tested in two different patients was provided by inter CC. SOM analysis can be used to interpret the activation of muscular systems, and by comparing the results of different individuals also to identify their TMJ health. Using the cross-correlation approach, one can find similarities in the sEMG data of different patients that can be used to provide clinically useful information. Such findings could be used to improve the clinical diagnosis of TMD and assess muscle activity during treatment.

1. Introduction

Multivariate data analysis methods can be applied to study many complex medical problems. Such methods can be used to better understand the behaviour of the human temporomandibular joint (TMJ) and to diagnose temporomandibular joint disorders (TMDs), which affect 5–12% of the human population [1]. The TMJ is the joint between the mandible and the temporal bone on the right and left sides of the head. The mandible performs complex movements that are a combination of translational and rotational displacements. The mobility of the joint influences not only the range of motion, but also the stability of the mandible. Any instability may cause discomfort or pain – this is known as temporomandibular joint disorder (TMD) [2,3]. Apart from pain or hindered jaw movements, joint clicking and popping during jaw motions can also indicate TMD. In advanced cases of disorders, surgical treatment may be necessary [4].

Improvement in TMD treatment requires a better understanding of TMJ behaviour. Forces that maintain jaw motion, acting on the lower jaw, are caused by active muscle forces, passive connective tissues (ligaments, tendons, bursa), and skeletal constraints [5]. To assess the behaviour of muscles acting at the TMJ during a given movement (jaw oscillation, mastication, talking, swallowing, or breathing), the electrical activation of the muscles can be measured by using electromyography (EMG) [6], which can be used in practice as either an invasive test (needle EMG) or a non-invasive test – surface electromyography (sEMG). This activation occurs during muscle contraction, which is evoked by a neural excitation transmitted from motor neurons to the motor units of the muscle.

Abbreviations: SOM, self-organising maps; sEMG, surface electromyography; CC, cross-correlation coefficient; TMJ, temporomandibular joint; TMD, temporomandibular disorder; MR, masseter right; ML, masseter left; TR, temporalis right; TL, temporalis left; RMS, root mean square; MVC, maximum voluntary contraction.

* Corresponding author.
E-mail address: kataszepi@pg.edu.pl (K. Szepietowska).

https://doi.org/10.1016/j.bspc.2021.103322
Received 24 May 2021; Received in revised form 20 October 2021; Accepted 2 November 2021

The features of EMG signals can be helpful to differentiate neuromuscular diseases as in [7]. Although EMG data can be applied to identify clinical problems that occur in the TMJ (neuromuscular diseases) [8–10], it has been argued that the information obtained from the EMG is insufficient for the diagnosis of TMD [11,12]. Furthermore, EMG data were used to differentiate between healthy patients and those with TMD in [13]. Moreover, it is also possible to use acoustic noise information for TMD detection [14]. The application of sEMG signals in the diagnosis and follow-up tests of patients with TMD was presented in [15]. However, an effective method of the classification of patients in clinical practice in the context of TMD diagnosis is still an open question.

One of the methods, that is being used in the analysis, is the cross correlation between two sEMG signals. In biomechanical studies, the cross-correlation was used to identify whether two time series of EMG data matched, e.g., in gait studies [16] and in the analysis of jaw muscle coordination during speech and selected movements [17]. Moreover, there are methods based on the theory of information, such as e.g., Mutual Information, Joint Entropy or Transfer Entropy methods, that can be applied as measures to compare biological signals [18]. In our study, we used cross-correlation to assess similarity between two series of processed sEMG (rectified and smoothed by using root mean square (RMS) algorithm). We presented our preliminary studies in [6]. It is worth emphasising that in the literature there is a lack of detailed reports describing the results of cross-correlation coefficients (CC) to assess similarities of two RMS patterns of sEMG (muscle activations) at the TMJ during opening, closing, protrusion, and retrusion for different skeletal classes.

Several machine learning approaches were developed to accurately and efficiently characterise EMG data, e.g., for neuromuscular disorders diagnosis, [19]. Classification methods such as decision tree algorithms [20], support vector machine [21], k-nearest neighbours algorithm [22,23] were also applied to biomedical signals, among other methods. Machine learning methods have also been proposed as efficient techniques for the identification of TMD based on cone beam computed tomography [24], or to predict clenching movements during mastication using a time-delayed and autoregressive artificial neural network (ANN) from sEMG data [25]. Several machine learning methods were applied to improve bruxism diagnosis, which involved extracting selected features from the sEMG of a masseter muscle [26].

Another type of artificial neural network is the self-organising map (SOM). Using SOM, large input datasets can be projected onto a two-dimensional (2D) representation known as a map [27]. This allows the relationships between the input data to be explored and their features assessed by encoding multidimensional characteristics into the said map. SOM has been used to detect anomalies in the synthetic and real EMG signals (erector spinae muscles) [28], to analyse the synergies of the trunk muscle [29], or to detect hand gestures in combination with the radial basis function network [30]. In addition, SOM was used to group the EMG signals of the biceps brachii muscles of 15 subjects into human percentile categories [31]. SOM was also applied to process pain questionnaire data in patients with TMD [32].

The presented research is a step towards a new (beyond skeletal class) classification of patients in terms of TMJ muscle activations. To address the weakness of existing approaches, we proposed using SOM and cross-correlation to assess the performance of the TMJ in patients by focusing on the selected muscles that act on the joint. The aim of this study is to apply these methods in clinical settings to classify patients in terms of the behaviour of their TMJ. This classification can be useful in the diagnostics of TMD as well as in mathematical modelling of the TMJ, and the results may be expanded towards semi-personalised musculoskeletal modelling. This will enable the definition of models corresponding to diverse groups of people with similar muscle performance. SOM is applied here to find clusters of sEMG results that are not based on trained data. The tested patients were classified according to the responses that their data elicited from the network.

This study will postulate two hypotheses:

1) SOM can be used to group patients based on the activation of all considered muscles (two temporalis and two masseters) expressed by RMS envelopes;
2) CC can be used to identify the instability of the TMJ by analysing the activity of the masseter, temporalis, ipsilateral and contralateral muscle pairs.

In order to address these hypotheses, the following questions are posed:

1) How are the sEMG data being clustered and what information can be extracted from them?
2) What is the similarity between pairs of sEMG signal envelopes of muscles in the form of a normalised RMS?

It should be emphasised that SOM processes all input data at the same time, whereas cross-correlation can only consider two signals at once. SOM therefore provides a more comprehensive overview of the behaviour of mastication muscles. We have already reported a preliminary study into the SOM analysis of sEMG in a conference abstract [33].

In this study, a group of patients underwent an sEMG examination. The acquired signals were then processed as inputs for the cross-correlation and SOM analyses (Fig. 1). Clusters of data are found and analysed together with the impact of each muscle activation on the outcome. Interpretation of SOM is provided to acquire information about similarities and dissimilarities between muscle activations among tested volunteers indicating similarities and dissimilarities in the condition of their TMJ.

2. Methods

2.1. Acquisition of biological signals

A group of 42 volunteers participated in Project 3D-JAW (The study of 3D temporo-mandibular joint (TMJ) model of bone-cartilage-ligament system mapping for effective commercialization of results in dental prosthetics, orthodontic and orthognathic surgery; POIR.04.01.02-00-0029/17). The purpose of our study was to group patients in terms of their muscle activations and therefore we selected only five volunteers from the Project 3D-JAW group who were classified as 'healthy' (without systemic diseases or the feeling of pain) on the basis of medical interviews and examinations carried out by a clinician. During the examination, however, three of the five volunteers did report mild issues with their temporomandibular joints. All the volunteers provided in writing informed consent in accordance with the procedures approved by Ethics Committee agreement No. KB/111/2018 (Medical University of Warsaw). Table 1 contains a description of the patients' gender, occlusion, as well as the mild TMJ issues reported by some of the patients during the examination. The examinations qualified all the subjects to have a subcutaneous fat layer in the lower range of thickness, which would not distort the sEMG signals.

To support the postulated hypotheses, we analysed the muscle activity of the volunteers, who were additionally classified by two independent clinicians according to their skeletal class (1st, 2nd, 3rd) and the symmetric anthropometric characteristics of the head-neck-trunk. Although there were only five volunteers, eight tests (recording sessions) were performed because three of them (Volunteers 1, 2 and 3) returned for a second examination session 5 months after the first. The resulting EMG datasets are denoted as entries I-VIII (Table 1), where I-V correspond to the first examination of all five volunteers, and entries VI, VII, and VIII correspond to the second examination of Volunteers 1, 3, 2, respectively.

Each of the volunteers underwent seven tests with opened eyes (vision on mode):

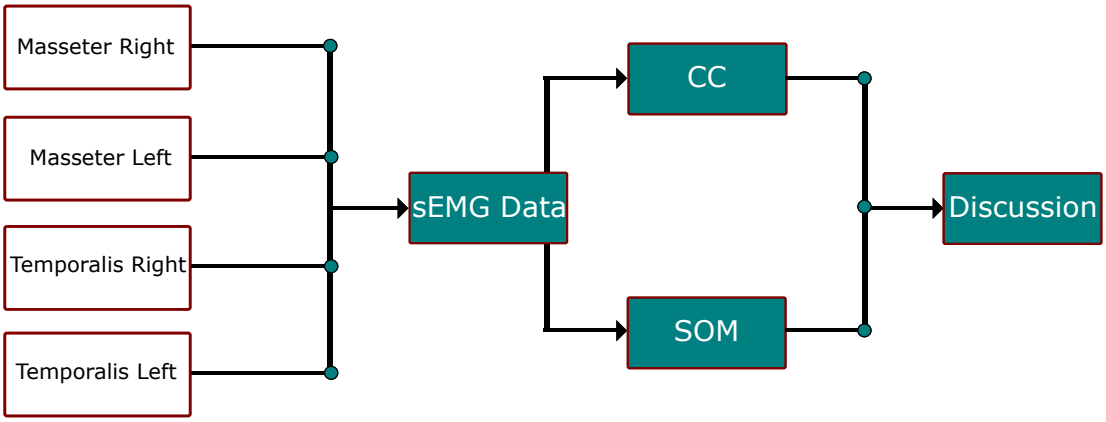

Fig. 1. Methodology flow chart.

Table 1
List of volunteers and their details.

Volunteers No.	Entry ID	Skeletal class	Gender	Occlusion	Height [cm]/weight [kg]/age	Self-reported mild issues
1	I, VI	1st	M	Normal	180/64/27	None
2	II, VIII	3rd	M	Anterior	171/63/20	Right disc blockage, increased muscle tension
3	III, VII	2nd	M	Deep bite	178/73/28	None
4	IV	3rd	M	Anterior	180/110/22	Muscle tension during chewing & yawning
5	V	1st	F	Normal	163/61/19	Clicking in the right TMJ (instability)

1) opening – closing of mouth;
2) protrusion – retrusion of mandible.

The mandibular movements were performed in the vertical position of the upper body, i.e. head-neck-torso. To perform open-close or protrusion-retrusion movements, the subject had to stabilize the position of their neck in relation to their torso and their head in relation to their neck. All the tests were performed with the open eyes (vision on mode). This mode was chosen because the sense of sight helps in performing upper body stabilisation and allows for smoother jaw movements (in the case of a healthy person) [34]. Motions were performed without prior instruction on the detailed performance to induce natural movement patterns.

To perform the biomechanical analysis, the kinematic data and the sEMG were synchronically measured . Kinematic data were used to define motion time intervals of open, close, protrusion and retrusion. Movement fragments (open, close, protrusion, retrusion) were selected on the basis of the velocity threshold of the jaw's motion, which was set

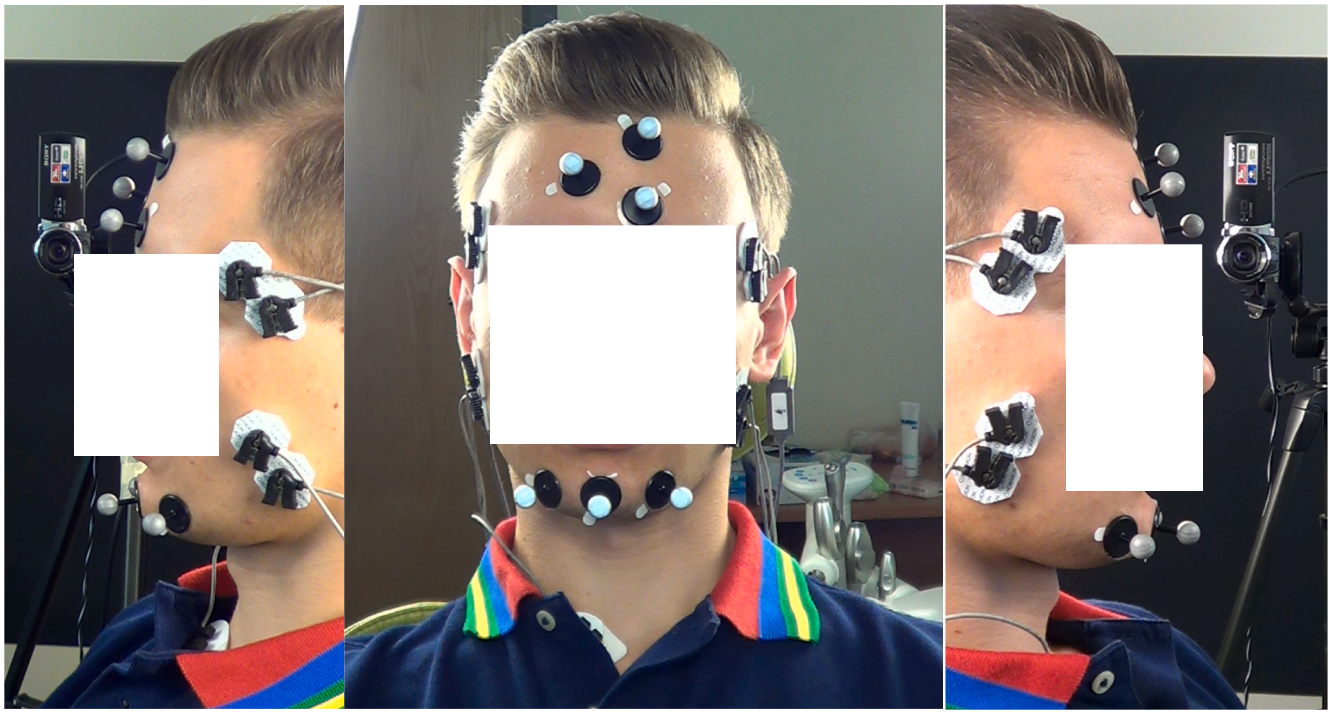

Fig. 2. Experimental setting. Volunteer with attached sEMG electrodes and passive markers: left – sagittal left view, centre – frontal view, right – sagittal right view.

up to 10 mm/s. Each identified motion fragment started when the velocity was higher than the velocity threshold and ended when the velocity was lower than the threshold.

Kinematic data were recorded by using the *Templo Contemplas* motion system, equipped with 3 cameras placed in front, on the left and right hand side of the subject. The experimental setting of the sEMG examination is shown in Fig. 2.

To measure the sEMG signal, the Noraxon MyoTrace 400 system (designed in accordance with IEC60601-2-40) and the Noraxon MyoResearch XP Clinical Edition software were used [35–38]. This wire system simultaneously collected data from four channels (with a 1000 Hz sampling rate) and transmitted them to a PC via Bluetooth. Each EMG channel was connected to a double electrode through the wire with a differential preamplifier. The first channel had an additional third electrode that was connected to a single reference electrode. The reference electrode was attached to the head of the medial clavicula during the test. The specification of each preamplifier was as follows: common mode rejection ratio (CMRR) exceeded 100 dB, input impedance was greater than 100MΩ, baseline noise was less than 1 μV RMS, base gain was 500 and input range was ±3.5 mV. Each EMG channel had an anti-aliasing filter set in the frequency range [10;500] Hz [39]. The analog-to-digital conversion of each EMG channel had a 16-bit resolution. Two types of disposable self-adhesive Ag/AgCl snap electrode (with electrolytic gel) were used:

1) Noraxon Dual Electrode: each circular conductive area diameter 1 cm (contact area covered by wet gel); inter-electrode distance 2 cm; -figure 8-shaped adhesive area 4 cm × 2.2 cm;

2) Noraxon Single Electrode: diameter of the circular conductive area 1 cm (contact area covered by wet gel); diameter of circular adhesive area of 3.9 cm; this electrode was used as a reference.

Double electrodes were glued to the skin on the bellies of the tested muscles and positioned along their fibers. Two pairs of muscles were tested: right Masseter (Muscle 1), left Masseter (Muscle 2), anterior part of the right Temporalis (Muscle 3) and anterior part of the left Temporalis (Muscle 4) [6]. SENIAM provides general recommendations about electrode location, but there are not specific references related to masseter and temporalis. Following [12] referring to electrode location, the electrodes were placed in the central part of the muscle bellies. The location of muscle bellies was determined by palpation during the jaw movements of the subject that activated the muscles examined. In case of the masseter, the belly of its anterior fibres was determined during the clenching of the teeth. In case of the temporalis, the belly of its anterior fibres was found during the opening-closing and clenching of teeth. The skin was prepared before testing by having the hair removed and being cleansed with alcohol (EcoLab Skinsept Pur Solution (46 g of ethanol + 27 g of isopropyl alcohol + 1 g of benzene alcohol)/100 g) to minimise impedance. In addition, to reduce the slight movement of the electrodes against the skin, all the electrodes and cables were secured against slipping with medical tape.

Using Noraxon MyoTrace 400, the raw sEMG were measured and recorded using MyoResearch XP Clinical Edition software. To process sEMG data, the raw sEMG data were rectified and smoothed by using the RMS algorithm with a 50 ms non-overlapping window (this RMS algorithm was integrated in the MyoResearch XP Clinical Edition software [36,37]). The cut-back of direct component (DC) was performed before running the signal processing (rectification and RMS in non-overlapping windows) with the use of the Noraxon MyoResearch XP Clinical Edition software setting called “zero offset”: 1) the EMG data were acquired during the initial interval while the tested muscles were in a relaxation state; next the DC component was determined (corresponding to background noise); 2) after measurement, the DC component was cut from the raw sEMG.

To assess muscle activation, processed sEMG data were transmitted to MATLAB and normalised by using an in-house code written in MATLAB with respect to the maximum voluntary contraction (MVC) data registered at the beginning of each test (maximum voluntary contraction was registered by asking the subject to clench their teeth as hard as possible over a 5–10 s interval). Muscle activations were assessed by assuming a 0.005 sEMG threshold (0.5% of the normalised scale, treated as an informative signal threshold) [12,40]. The value of the electromechanical delay (50 ms) was established according to [41]. This delay reflects that muscle contraction happens after activation, i.e., these two phenomena (activation and contraction) do not happen at the same time. The time segments for each repetition of the movement were slightly different (human movements are rarely repeatable in time). The elapsed time of each examination (stride) was normalised (to 100%) and given as a percentage of the total time of movement. This time normalisation was similar to the gait analysis normalisation presented in [16]. The sampling of each stride (repetition of movement) was interpolated and resampled to 1000 points. Each muscle activation was computed as a mean of normalised RMS envelopes from the seven tests. For the sake of simplicity, the normalised RMS envelopes of the muscles' sEMG will henceforth be called muscle activations or sEMG data. To sum up, our final processed EMG data contains 1000 resampled points corresponding to 100% of a given movement.

Analysis was performed for different phases of motion to capture different muscle activations during different phases of motion. Based on acquired kinematic data (acceleration and velocity), three phases of the jaw motion were defined: 1) acceleration phase – 0–30% of the motion (300 resampled points); 2) middle phase – 30–70% of the motion (400 resampled points); 3) deceleration phase – 70–100% of the motion (300 resampled points).

2.2. Cross-correlation

The cross-correlation approach allows one to identify the similarity of two time series by assessing the cross-correlation coefficient (CC) and/or plotting the estimated cross-correlation of two signals (cross-correlograms) [42–44]. We used the MATLAB function *xcorr* to assess the cross-correlation between two RMS pattern of sEMG (muscle activations) and its sub function *coeff* to assess the CC. In line with the aim of this study, we evaluated the CC in two ways:

1) the intra cross-correlation approach was used to match two muscle activations (RMS envelopes) of the same volunteer: right, left, ipsilateral and contralateral pairs of muscles of each subject;
2) the inter cross-correlation approach was applied to match activations (RMS envelopes) of the same muscle of a selected volunteer with the RMS pattern of sEMG of a reference volunteer (Entries I, II and III). The inter CC assessments were carried out to compare the CC results with the SOM classification results, where all the muscles were considered simultaneously in a single analysis (Section 4).

The similarity of the time series was assessed according to the following scale of the CC value (CC scale):

1 – good (0.97 – 1.00],
2 – moderate (0.94 – 0.97],
3 – fair (0.90 – 0.94],
4 – weak ≤ 0.9.

Considering symmetrical motion with respect to the sagittal plane, we assume that the instability of the TMJ occurs when a low similarity (for the intra CC analysis) is observed between:

a) muscles 1&2;
b) muscles 3&4;
c) ipsilateral muscle pairs 1&3 and 2&4;
d) contralateral muscle pairs 1&4 and 2&3.

2.3. Self-organising maps

The self-organising maps model used in this study is an unsupervised learning algorithm [27]. This type of classification method is a pattern recognition technique based on unlabelled datasets, in contrast to a

supervised algorithm, which needs a significant amount of labelled data to train the model and then test it on the unseen input. SOM enables the visualisation of nonlinear relations between multidimensional data points using a map of neurons. It reduces the dimensionality of the data, but preserves and represents the topographic relationships between the data (Fig. 3) [45]. The SOM architecture consists of a single layer of nodes (neurons) formed in a two-dimensional grid of neurons to which the input data are presented. Let $\boldsymbol{x} \in \mathbb{R}^P$ be the P-dimensional input vector and $\boldsymbol{w}_i$ be a P-dimensional vector of weights associated with the i-th neuron. Each component of the weight vector corresponds to a component of the input vector. The algorithm starts with all weights being initialised with a random number between 0 and 1 [27]. During the training phase, input vector **x** is presented to the network of all the neurons and only the neuron which is found to be the most similar to this input is stimulated and identified as the Best Matching Unit (BMU) in the network. The BMU is thus the neuron which minimises the Euclidean distance to the input vector **x**:

$$\mathrm{BMU} = \underset{i}{argmin}\{\|\boldsymbol{x} - \boldsymbol{w}_i\|\} \tag{1}$$

The weights of neighbouring neurons are then updated according to the neighbourhood function [46], distributing similar data locally around the BMU. The process is repeated for all data input samples that are presented to the network. A detailed description of the SOM algorithm can be found in [46].

After the training, the organised output map of neurons contains a representation of the input data. To visualise the clustering of the data, the U-matrix (unified distance matrix) method can be used [47]. The U-matrix represents the Euclidean distance between the weight vectors of neighbouring neurons. Neurons with short distances between each other form clusters (dark colours) and neuron weights with long distances between each other define the cluster boundaries (bright colours) (Fig. 3).

Information about input datasets and network settings are shown in Table 2. In our study, the input vectors contained processed sEMG signals. The dataset used for the training of a single map was composed of sEMG sampling points corresponding to a given phase of every motion (open, close, protrusion, or retrusion) of all the volunteers during the recording sessions (entries) (see Fig. 4). The four variables ($P = 4$) reflected the four muscles examined. 1000 data points of sEMG (resampled points corresponding to 100% of motion) were divided according to the assumed motion phases, i.e. m (number of samples of one entry of one phase) equals 300 in the acceleration phase (30% of motion), then 400 in the middle phase (40% of motion) and again 300 in the deceleration phase (30% of motion). Therefore, M – the number of points in the dataset – equals m times L, where L is the number of entries (labels), and here $L = 8$. By adding label information, the procedure was adapted to provide supervised visualisation and used to interpret the clustering of data [27,45]. A vector that defines the labels was provided as a numerical column vector. Eight labels can therefore be distinguished as entry IDs: I, II, III, IV, V, VI, VII, VIII, respectively. Note that the labels were not used during the training phase but only after training to identify where the clusters for each grouped samples were organised.

The size of the network (map grid) – defines the number of neurons N used for training [45]. In our study, we adopted a general rule described in [45], according to which the value of N was around $N = 5\sqrt{M}$, where M was the number of samples in the dataset. The ratio of the side lengths of a given map was determined according to the ratio between the two largest eigenvalues of the input data matrix [48]. All training was performed in batch mode, where the entire sample set was presented to the network and the winning neurons were found. Then the map weights were updated, affecting all samples. This is in contrast to sequential training, where at each training stage, samples are presented to the network, one at a time, and the weights are updated according to the winning neuron. The latter method is more time consuming and error prone. The number of training epochs – that is, the number of times each sample is introduced into the network until the map converges – was set individually for each analysis [45]. In this study, an open source toolbox – SOM Toolbox for MATLAB [48] was used.

3. Results

In this study, cross-correlations and SOM analyses for the three defined phases of each motion were performed. Processed sEMG data (normalised RMS envelopes/muscle activations), obtained during the following jaw motions – opening, closing, protrusion, and retrusion – were taken as an input to these analyses. The activations (RMS envelopes) of the considered muscles are presented in Figs. 5–8.

3.1. SOM results

The SOM results are presented in Figs. 9–11 and in Table 3. More detailed information on the acceleration phase of the opening motion is provided as an example to explain the method. The results of the other analyses are included in the attached supplementary material.[1] A U-matrix presenting dimensionless values and a labelled map are shown in Fig. 9. The clusters formed in an output space are labelled with the entry IDs. The U-matrix represents the Euclidean distance between the weight vectors of neighbouring neurons. In addition to U-matrix maps, it is interesting to note the differences between each component plane of the SOM (Fig. 10). Here, a component plane also consists of dimensionless values, and it depicts the weighted average value for one variable (muscle) of the input data. Thus, conclusions about a single input variable can be drawn. What follows, one can evaluate the significance of each component for classification and gain a general insight into the analysed multidimensional data. Figs. 9 and 10 visualise the same SOM training so that the map units (hexagons) correspond to each other by location and represent the same neurons.

In Fig. 9, clusters corresponding to Entry II are scattered throughout the map. That may be associated with higher variability in the values of all 4-dimensional activation data points represented by RMS envelopes (Figs. 5–8). Furthermore, it should be noted that the data samples corresponding to Entry I are gathered in small numbers of neurons that form a tight cluster. This can be explained by the fact that all activation data points in case of Entry I do not change much over the time of the motion on the RMS envelopes.

The groups of neurons corresponding to Entries IV and V are the most distant from the neighbouring clusters. This means that the weights of neurons are significantly higher on specific variables, compared to the low weights of others Entries (Fig. 10, see Masseter Left and Temporalis Right variables), which cause their clusters to be clearly separated from others.

Analysing the SOM results of all the studied motion phases (Fig. 11 and Table 3) including those presented in supplementary material A, the following observations were made:

- Entry I has low weight values for every muscle variable in every motion (see supplementary material A for Fig. A.1–Fig. A.12).
- Entry II has the highest weight values for the masseter right (MR) during all motions. Scattering of clusters throughout the map at the acceleration phases of opening and closing motions (Fig. A.1, Fig. A.4) is observed.
- Entry III has high weight values of the masseter left (ML). In the slowing down phase of retrusion, Entry III also has a wide range of weight values for MR and ML (Fig. A.12).
- Entry IV has considerable data separation from other clusters. It has high weight values for ML and temporalis right (TR) (Fig. A.1–Fig. A.12) and a wide range of weight values for temporalis

[1] All SOM results are in supplementary material (A – results of SOM analysis) submitted along with this manuscript, see Appendix A Supplementary Data.

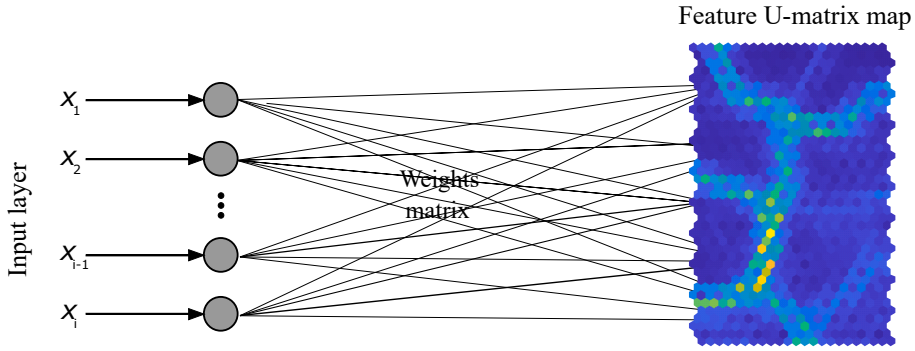

Fig. 3. SOM algorithm operation. The colours on the U-matrix map represent the Euclidean distances between neighbouring neurons.

Table 2
Network settings for datasets representing given phases of motions.

Dataset	No. of samples (*M*)	Map Size	No. of Neurons (*N*)	No. of Training Epochs
Opening 0-30%	300x8=2400	[22x11]	242	200
Closing 0-30%	300x8=2400	[19x13]	247	200
Protrusion 0-30%	300x8=2400	[22x11]	242	200
Retrusion 0-30%	300x8=2400	[20x12]	240	200
Opening 30-70%	400x8=3200	[22x13]	286	250
Closing 30-70%	400x8=3200	[22x13]	286	250
Protrusion 30-70%	400x8=3200	[24x12]	288	250
Retrusion 30-70%	400x8=3200	[22x13]	286	250
Opening 70-100%	300x8=2400	[18x14]	252	200
Closing 70-100%	300x8=2400	[20x12]	240	200
Protrusion 70-100%	300x8=2400	[19x13]	247	200
Retrusion 70-100%	300x8=2400	[20x12]	240	200

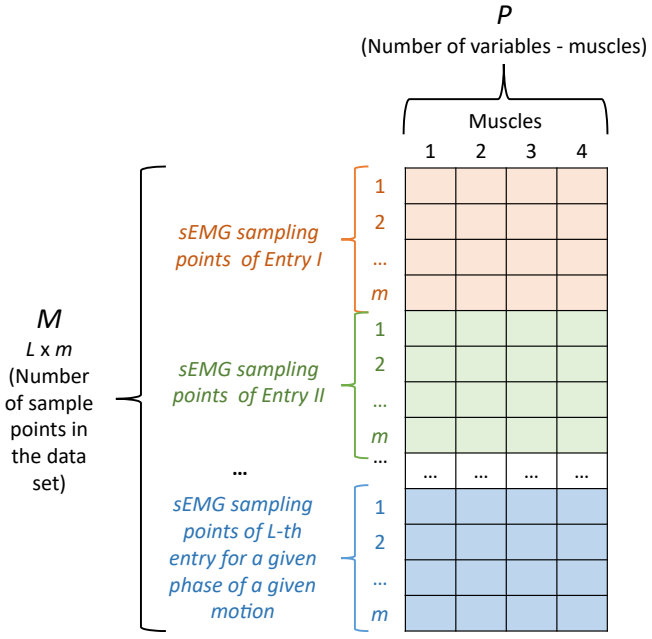

Fig. 4. Dataset input to the SOM.

left (TL) in the opening motion and ML in the closing motion (see Fig. A.1–Fig. A.6).

- Entry V has more pronounced cluster separation than other entries with variable, from medium to high weight values for ML (Fig. A.1–Fig. A.12).
- Entry VI has medium values on every variable in every motion and phase (Fig. A.1–Fig. A.12).
- Entry VII has values varying from medium to high during all motions for ML and TL (Fig. A.1–Fig. A.12) and also a wide range of values for MR during retrusion (Fig. A.10–Fig. A.12).
- Entry VIII has high weight values for TL in every motion and phase (Fig. A.10–Fig. A.12) a wide range weight values for MR (Fig. A.7–Fig. A.9), for ML during protrusion (Fig. A.9) and for ML (Fig. A.10) during retrusion.

A summary of the clustering of entries (the data that were found to be the most similar to each other) can be found in Table 3 and observed on the appropriate U-matrix maps (Fig. 11). It should be noted that no neuron had identical samples to those of other entries, which would indicate high similarity in muscle activation (RMS envelopes) of the volunteers. Nevertheless, the similarity between volunteers can still be observed in the maps where they form clusters without clearly defined borders, that is, when the distance between the nodes is small (dark colour). Clear boundaries between the clusters are defined with bright colours, which means a large Euclidean distance between neighbouring neurons. There is no threshold set for the Euclidean distance in the analysis. The entries that clustered together in specific phases of motions and also the maximum Euclidean distances between neighbouring neurons are presented in Table 3.

3.2. Cross-correlation results

Intra CC results are presented in Table 4 and the supplementary material B[2] that were obtained on the basis of the intra CC. The results are presented as a percentage of entries assigned to each skeletal class in every tested phase of motion that corresponds to a given CC scale level by revealing a stronger or weaker correlation. The plots of estimated intra cross-correlograms for the first phase of opening motion (0–30%) for all entries are shown in Figs. 12 and 13 (other correlograms are given in supplementary material D). The value of the lag in every analysis was 0.

In reference to the detailed inter CC results presented in supplementary material C, the integrated results are presented in Table 5. These results were obtained on the base of inter CC that were scored according to the CC scale, i.e. indicating the level of inter CC between

[2] All intra and inter CC results are in supplementary material B (intra CC results), C (inter CC results) and D (Intra cross-correlograms) submitted along with this manuscript (see Appendix A Supplementary Data).

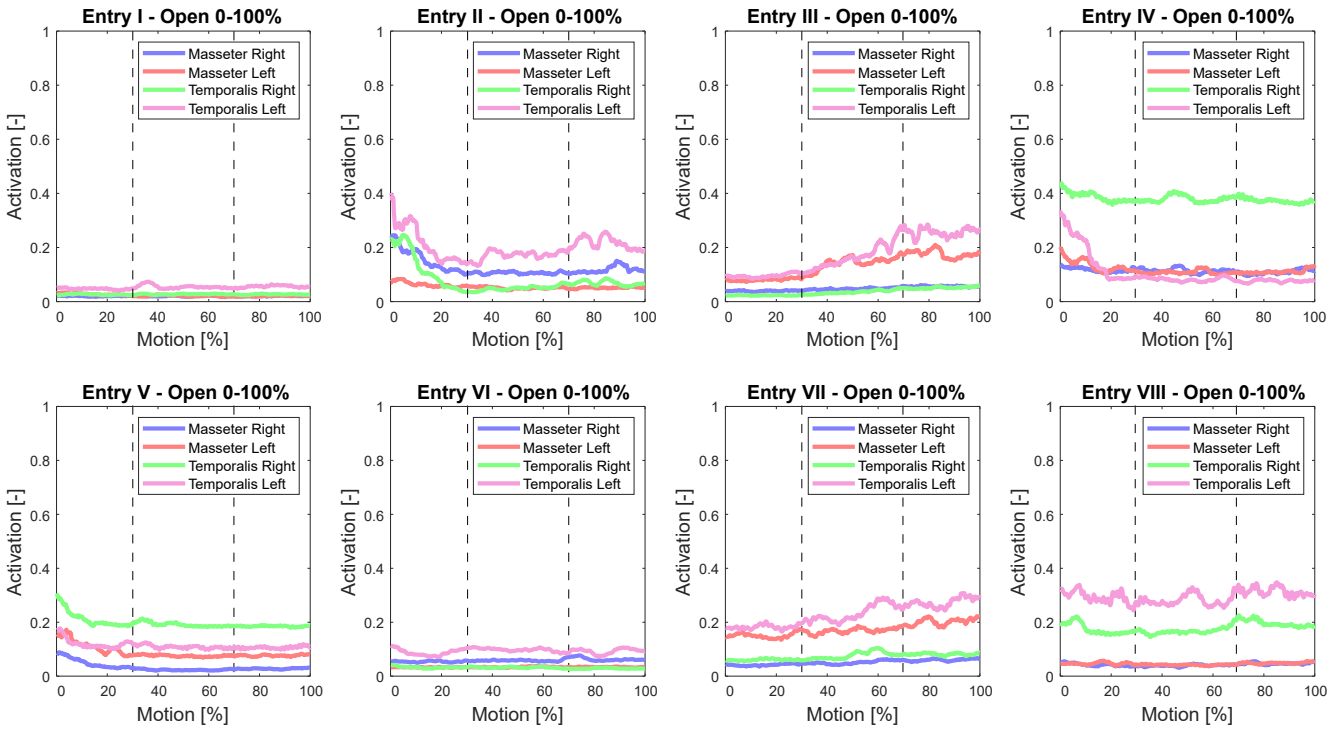

Fig. 5. RMS envelopes of the muscle sEMG during jaw opening with outlines of motion phases (grey dashed lines): acceleration phase 0–30% of motion, middle phase 30–70%, deceleration phase 70–100%.

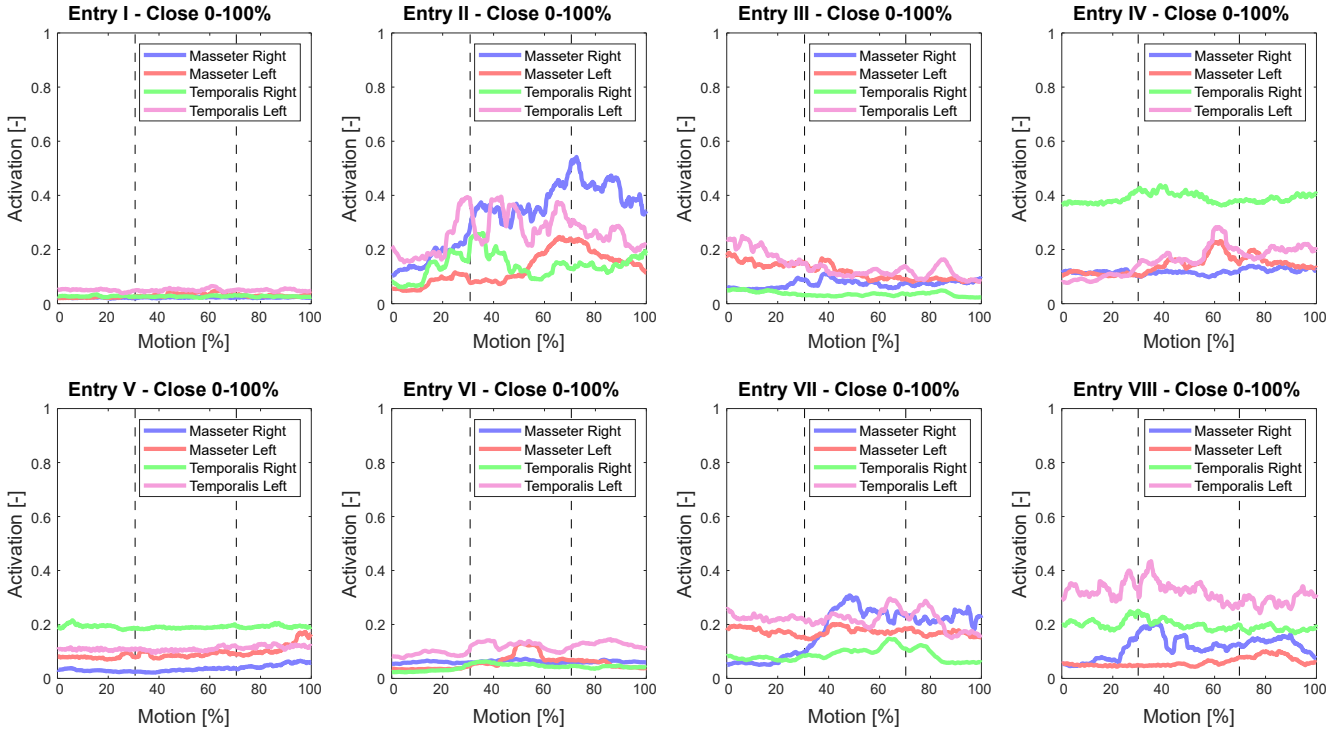

Fig. 6. RMS envelopes of the muscle sEMG during jaw closing with outlines of motion phases (grey dashed lines): acceleration phase 0–30% of motion, middle phase 30–70%, deceleration phase 70–100%.

RMS envelopes (activations) of corresponding muscles in a pair of subjects.

4. Discussion

In this study, we have analysed SOM results to identify data clusters on U-matrix maps with assigned labels, assessed the cluster borders and the distances between the clusters, evaluated the impact of specific

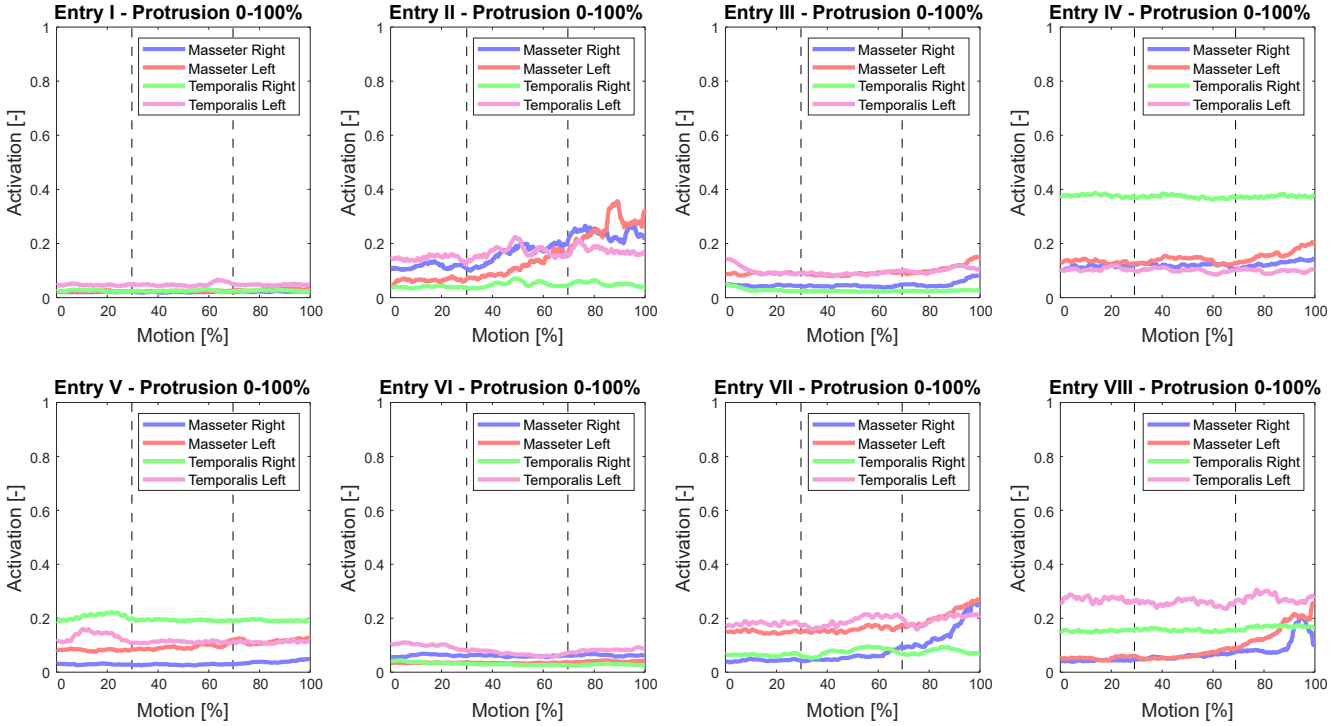

Fig. 7. RMS envelopes of the muscle sEMG during jaw protrusion with outlines of motion phases (grey dashed lines): acceleration phase 0–30% of motion, middle phase 30–70%, deceleration phase 70–100%.

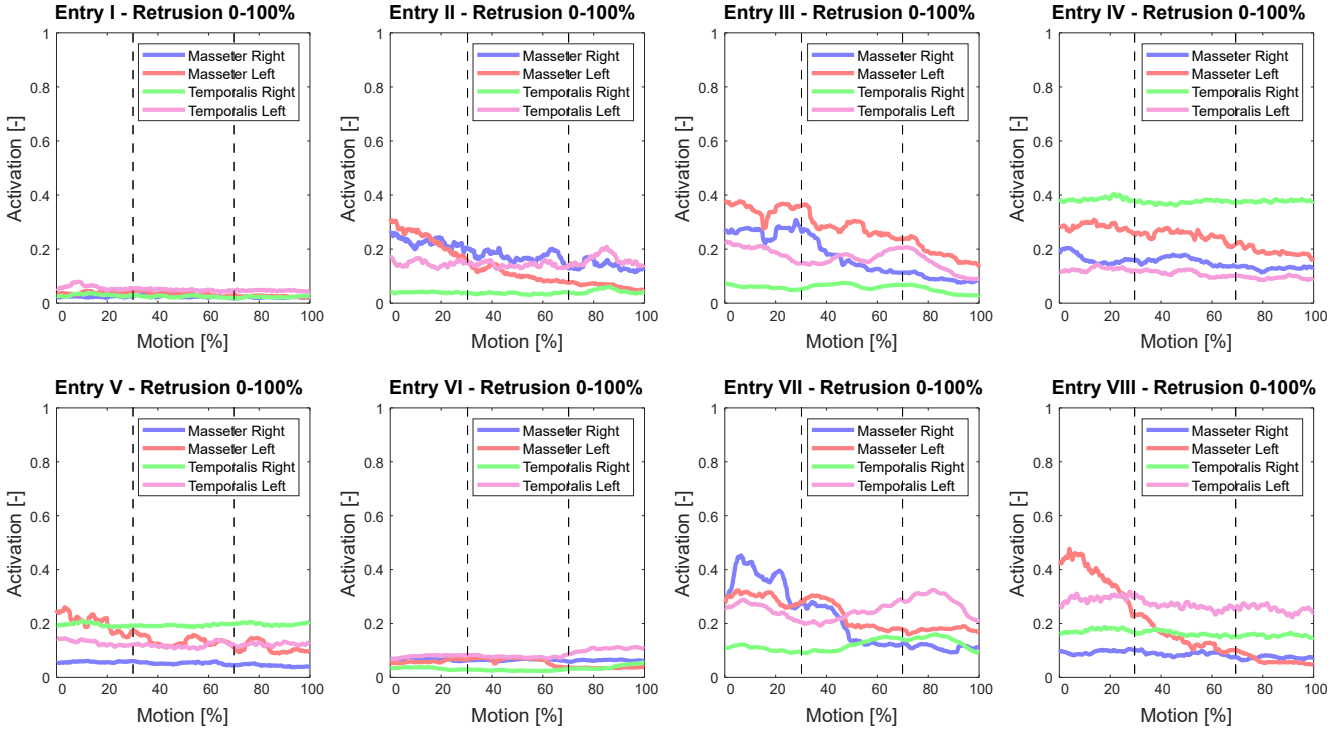

Fig. 8. RMS envelopes of the muscle sEMG during jaw retrusion with outlines of motion phases (grey dashed lines): acceleration phase 0–30% of motion, middle phase 30–70%, deceleration phase 70–100%.

variables on feature maps and compared the information from the SOM results with visual inspections of muscle activation expressed by RMS pattern of sEMG (input data). The following SOM results provide satisfactory interpretation of muscle activity and consequently may have clinical significance:

1) Clustering of entries together implies the similarity of their input muscle activation, which may indicate a similarity in their TMJ health condition;

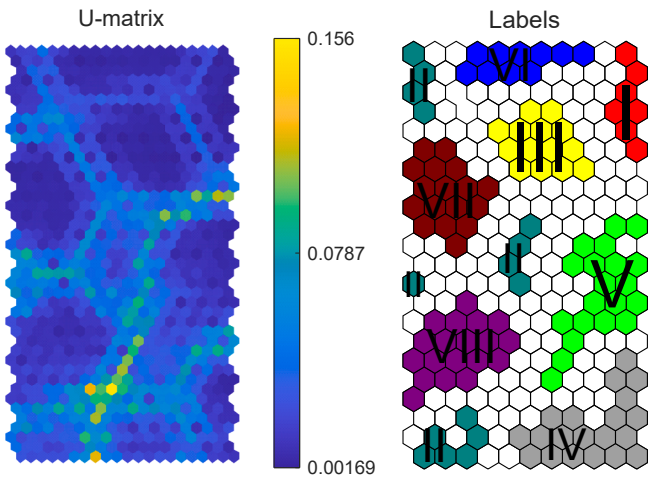

Fig. 9. SOM results for the acceleration phase of opening motion (0–30%): U-matrix map of TMJ muscles processed sEMG data (left) with colour bar values representing Euclidean distance between neighbouring neurons; map with labels (marked with Roman numerals) corresponding to Entry ID (right).

2) A considerable separation of the group of entries from the other implies a dissimilarity in the activation of the input muscle, which may indicate differences in their health condition;
3) The higher the number of neurons corresponding to an entry, the more variable the sEMG data (input) of this entry. A tight cluster of data that corresponds to one entry with a small number of neurons indicates the similarity of sEMG samples.
4) When an entry is divided into several clusters scattered across the map, this implies high dissimilarities between the samples of muscle activation and may indicate a type of disorder.

However, such conclusions regarding TMJ need to be confirmed clinically in a future study with a larger number of entries.

On the basis of the aforementioned remarks, the following detailed observations can be made. First, the SOM results did not show clustering corresponding to the skeletal class. Instead, the data of the Entries I and III were found to be similar to the muscle activation data (RMS envelopes) of the same volunteers collected in Entries VI and VII, respectively, five months after the first examination (Table 3), which indicates that SOM is a good method for the detection of similar muscle activation.

Furthermore, the similarity in the data found between Entries III and VI (Fig. 11, Table 3), especially during the middle phase of the closing motion, indicates a possible similarity in the activation of muscles.

Taking into account all the results for all the entries (supplementary material A), it can be observed that in the case of the opening motion, the variable that yielded the highest responses (weight values) was the temporalis right (Fig. A.1–Fig. A.3). In the case of the closing motion, the highest weight values were found for the masseter and temporalis right (Fig. A.1–Fig. A.6). For the protrusion motion, the highest weight values were for the temporalis right (Fig. A.7–Fig. A.9). For the retrusion motion, the highest weight values were for the temporalis right throughout the whole motion (Fig. A.10–Fig. A.12) and partly for the masseter left (0–70%, Fig. A.10–Fig. A.11).

Compared to the opening-closing motion, protrusion-retrusion provided more pronounced clusters. It may be explained by the fact that protrusion-retrusion are not every day movements. Therefore, examination of the muscles responsible for protrusion and retrusion may be considered a better grouping factor for SOM analysis. However, higher inter CC were found in the case of protrusion-retrusion than in the case of opening-closing.

It should be noted that in the first phase of opening (acceleration phase), the inter CC between Volunteer 2 and other volunteers are in the range defined as weak (inter CC < 0.9) for the right temporalis (Table 5), whereas in the SOM, Entry II (Volunteer 2) is divided into smaller groups, scattered around the map between other entries (Fig. 9). Therefore, both methods indicate an issue in the case of this subject. Indeed, Volunteer 2 reported mild issues with the TMJ.

The data for volunteers 2 and 3 had a high number of neurons and a wide range of weight values, which cluster with a loose consistency on the maps (Fig. A.1, Fig. A.10–Fig. A.12). This may indicate variability in data and, as a result – variable activity of TMJ muscles in both volunteers. The similar responses of the SOM and input data regarding the two volunteers may indicate similar TMJ problems. Thus, the mild problem reported by Volunteer 2 may also occur with Volunteer 3.

The data for Volunteer 1 are grouped with a low number of neurons (tight cluster) with low weight values. This represents similar behaviour of the tested muscles with low variability of the EMG data throughout the whole motion. The same can also be seen in the RMS envelopes (Figs. 5–8).

The best separated clusters for every motion correspond to Volunteer 4 (Fig. 11). This is due to the highest input values from temporalis right in comparison to the rest of the dataset (Fig. A.1–Fig. A.12). Entry IV is well separated (Fig. 11) even in cases where the inter CC between RMS envelopes (activations) of all four muscles of this volunteer and those of the reference volunteers is good (Table 5 and supplementary material C). The cluster for Entry V is also clearly separated from the rest. Since this volunteer reported a clicking sound in the right TMJ, a short data distance to this cluster of a potential new subject may indicate similar TMJ conditions. Entries IV and V are the cases of people with

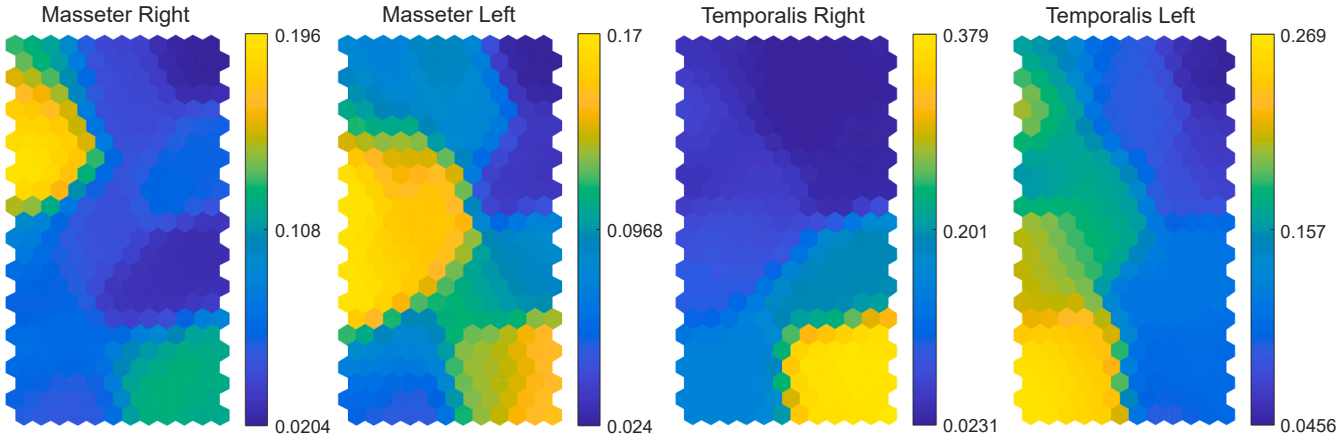

Fig. 10. SOM results for the acceleration phase of opening motion (0–30% of motion): component planes of each variable (corresponding to TMJ muscles) with colour bar values representing weighted average of data samples in neurons.

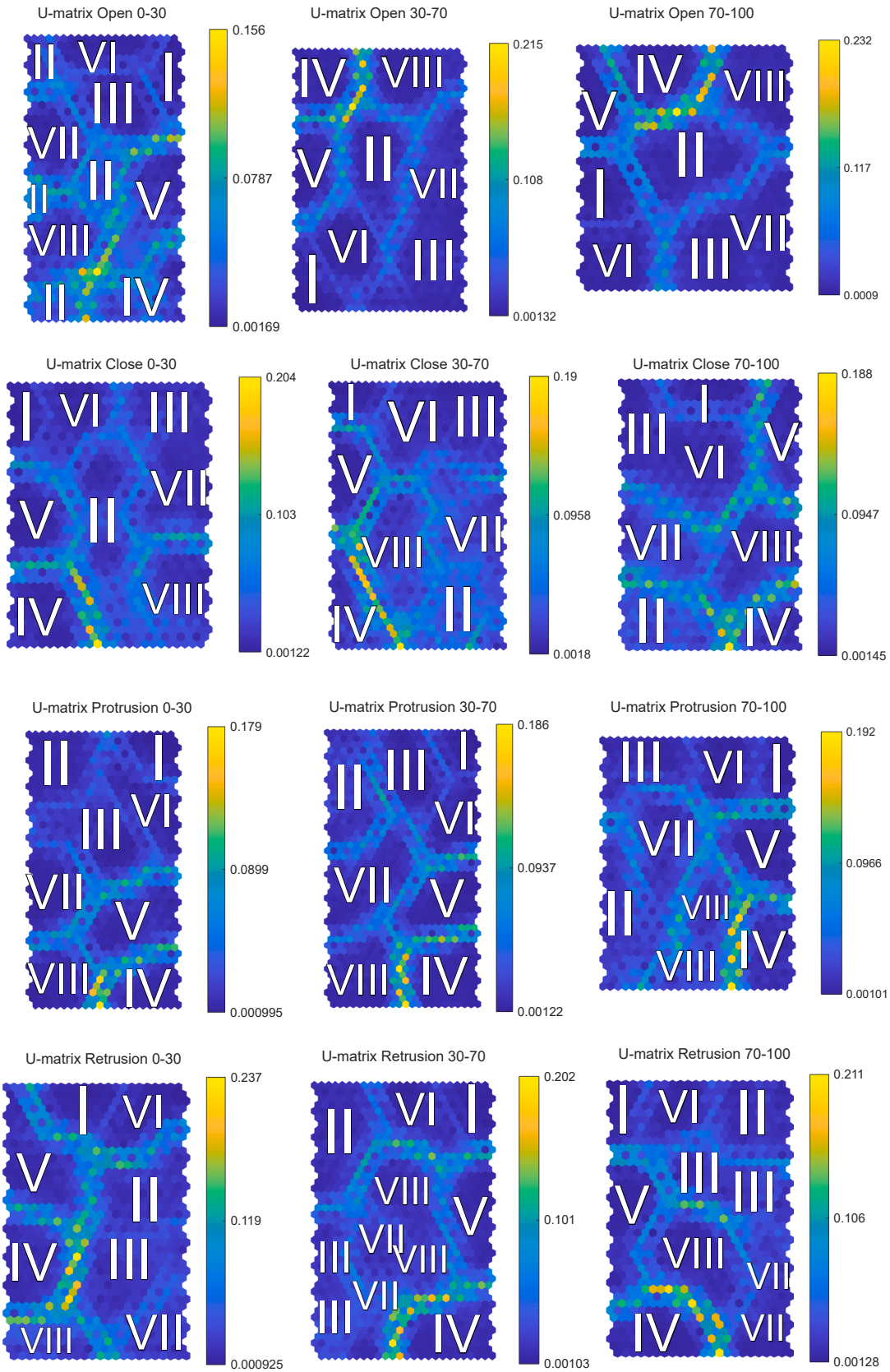

Fig. 11. SOM U-matrix maps of TMJ muscles of processed sEMG data for examined motions in three phases. Colour bar values represent Euclidean distance between neighbouring neurons; labels (Roman numerals) correspond to Entry IDs.

Table 3
SOM U-matrix results.

Motion	Entries clustered together	Max. Euclidean distance between weight vectors of neighbouring nodes
Open 0–30%	–	0.156
Open 30–70%	III & VII	0.215
Open 70–100%	III & VII	0.232
Close 0–30%	III & VII	0.204
Close 30–70%	III & VI, II & VII	0.190
Close 70–100%	III & VI	0.188
Protrusion 0–30%	–	0.179
Protrusion 30–70%	–	0.186
Protrusion 70–100%	I & VI	0.192
Retrusion 0–30%	II & III, I & VI	0.237
Retrusion 30–70%	VII & VIII	0.202
Retrusion 70–100%	III & VII	0.211

Table 4
Percentage of Entries in Each Skeletal Class that correspond to given level of CC scale calculated on the base of intra Cross–correlation coefficients for Each Pair of Muscles during Opening Motion Acceleration Phase (0–30% of Motion).

Pair of Muscles	Level of CC	1st Skeletal Class – three entries [%]	2nd Skeletal Class – two entries [%]	3rd Skeletal Class – three entries [%]
1-2	Good	100	100	100
	Moderate	0	0	0
	Fair	0	0	0
	Weak	0	0	0
3-4	Good	100	100	33
	Moderate	0	0	33
	Fair	0	0	33
	Weak	0	0	0
1-3	Good	100	100	66
	Moderate	0	0	33
	Fair	0	0	0
	Weak	0	0	0
2-4	Good	100	100	66
	Moderate	0	0	33
	Fair	0	0	0
	Weak	0	0	0
1-4	Good	66	100	66
	Moderate	33	0	0
	Fair	0	0	33
	Weak	0	0	0
2-3	Good	100	100	66
	Moderate	0	0	0
	Fair	0	0	33
	Weak	0	0	0

asymmetric muscle activation and overloaded right TMJ. It is characteristic of right-handed volunteers. Since Volunteer 4 is left-handed, such a response may indicate a hidden pathology in the right TMJ and the need for further diagnosis. The activity of the TR is probably less highlighted in the case of Volunteer 5 due to the different gender and skeletal class.

It should be noted that the input to the SOM contained the data of all five volunteers. Therefore, the interpretation of the SOM results can be compared with other volunteers in the input. On the other hand, the inter CC compares only a pair of muscles in two volunteers. The intra CC, in turn, considers only one volunteer and provides a measure of similarity between the RMS envelopes (activations) of pairs of muscles in that one volunteer.

The cross-correlation results for RMS pattern of sEMG (muscle activity) were discussed with regard to identifying the instability of the TMJ within skeletal classes and between them. Based on the intra CC results, we found the following:

1) The 1st skeletal class entries had the highest similarity during all phases of the opening/protrusion/retrusion motion. In the case of the closing motion, these volunteers demonstrated the highest similarity during the acceleration and slowing down phases and good to moderate similarity in the middle phase;
2) The 2nd skeletal class entries had the highest similarity during all phases of the opening/protrusion/retrusion motions. In the case of the closing motion, these volunteers had the highest similarity during the middle and slowing down phases and good to moderate similarity in the acceleration phase;
3) The 3rd skeletal class entries had a good to moderate similarity during the protrusion and retrusion motions. The most differentiations were observed in the opening motion of the acceleration phase and, for the closing motion, in the acceleration and middle phases.

Analysing the intra CC of ipsilateral muscle pairs 1&3 and 2&4, we found that:

1) the highest similarity appeared in all phases for the 1st – 2nd skeletal class in the opening motion and for the 1st skeletal class in the protrusion and retrusion motions;
2) a moderate to good degree of similarity appeared for the 3rd skeletal class during the opening and retrusion motion, and the 1st and the 2nd skeletal class during closing. The greatest differences were found for the 3rd skeletal class during the closing motion.

Considering the intra CC of the contralateral muscle pairs 1&4 and 2&3, we observed the following:

1) the highest similarity was for the 2nd skeletal class in the opening motion and for the 1st skeletal class during protrusion and retrusion;
2) good to moderate similarity appeared for the 1st skeletal class in the opening motion, the 2nd skeletal class during the closing and protrusion, and the 3rd skeletal class during retrusion.

The study is based on the examination of healthy subjects with jaw musculoskeletal symmetry. The motions performed were symmetrical in the sagittal plane; therefore, it could be expected that each subject would activate the muscles in the similar way. Hence, the intra CC were expected to be high, in case of individuals without TMJ instabilities. Indeed, many of the obtained intra CC were within the range denoted as good. Referring to the inter CC, it was observed that many of these coefficients were also in the good range, which could be a result of examining healthy individuals. Nevertheless, some results were still observed in the moderate, fair and weak ranges (see supplementary materials B and C).

The advantage of the SOM approach is the possibility of grouping patients in terms of muscle activation regardless of other existing classifications. Supervised algorithms are useful in disease diagnosis, as

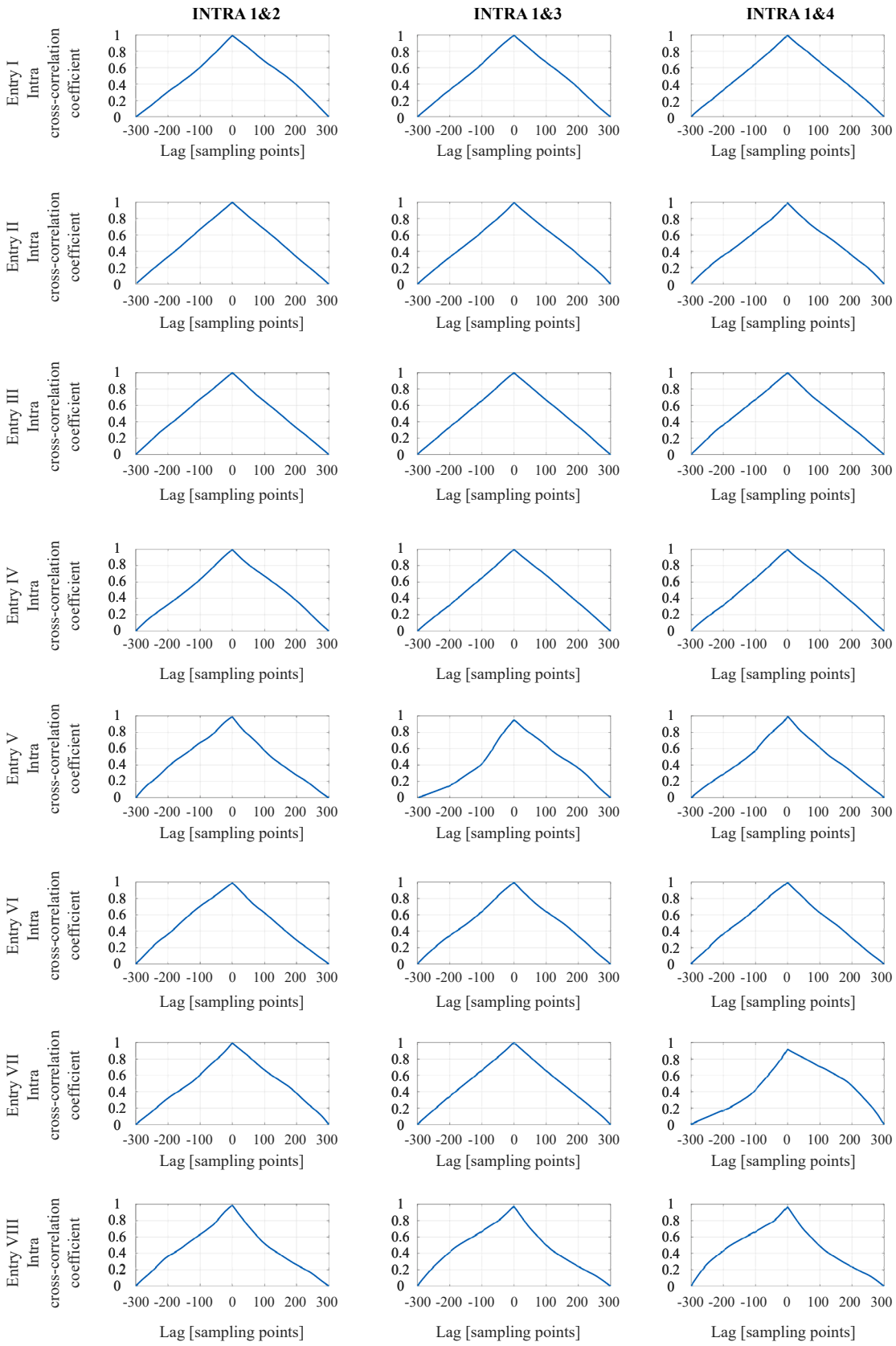

Fig. 12. Intra Cross-Correlogram for acceleration phase (0–30%) of opening motion for all entries. Vertical axis – cross-correlation coefficient between RMS envelopes for muscles 1&2, 1&3, 1&4; horizontal axis–time given in resampled points.

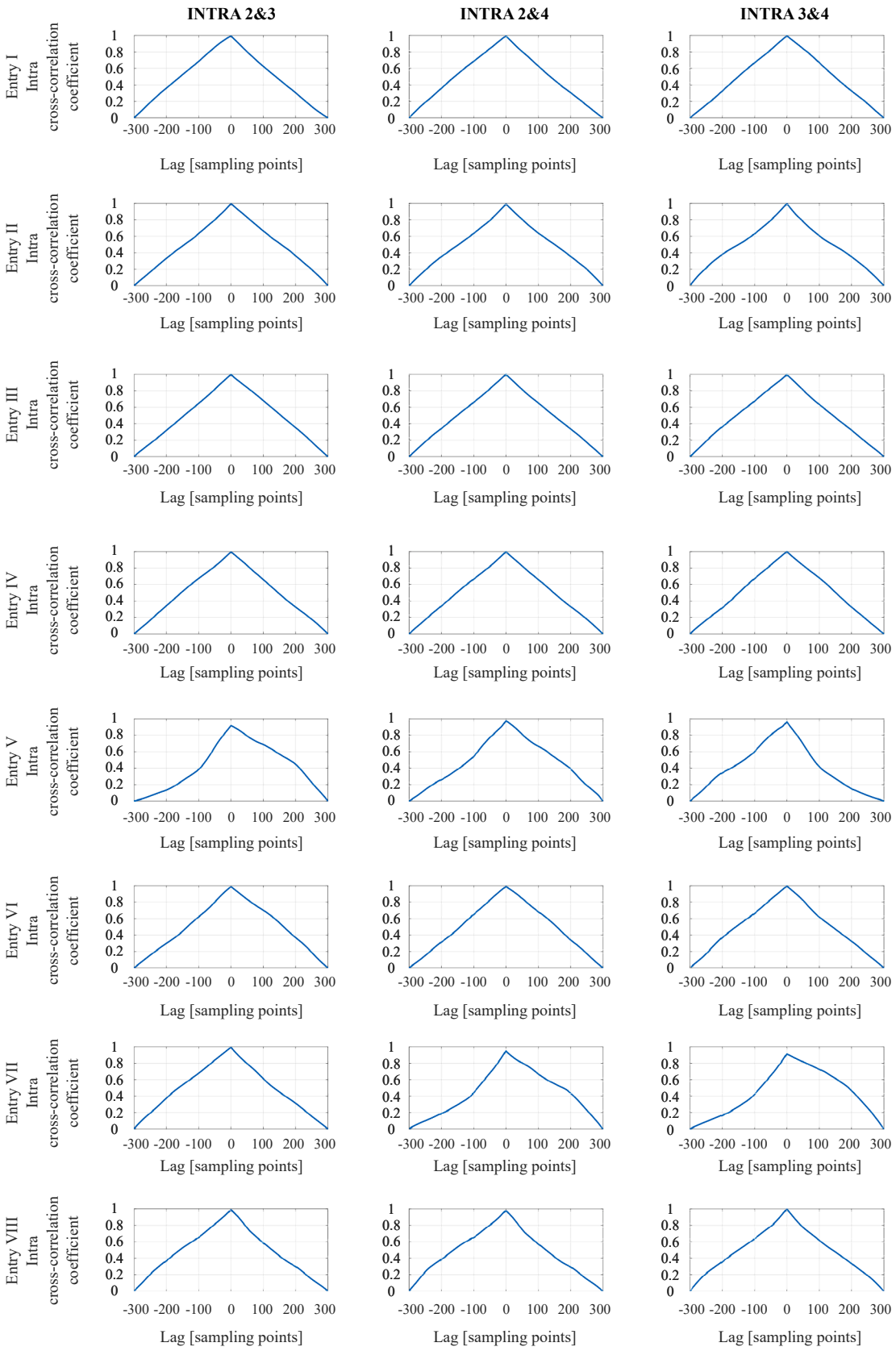

Fig. 13. Intra Cross-Correlogram for acceleration phase (0–30%) of opening motion for all entries. Vertical axis – cross-correlation coefficient between RMS envelopes for muscles 2&3, 2&4, 3&4; horizontal axis–time given in resampled points.

Table 5
CC scale level of inter Cross-correlation coefficients calculated between Corresponding RMS Envelopes of Pairs of Subjects (Entries). Opening Motion, Acceleration Phase (0–30% of Motion).

Muscle ID	Entry ID	Base Entry I	Base Entry II	Base Entry III
1	I	-	2	1
	II	2	-	2
	III	1	2	-
	IV	1	1	1
	V	3	1	3
	VI	1	2	1
	VII	1	2	1
	VIII	1	1	1
2	I	-	1	1
	II	1	-	1
	III	1	1	-
	IV	1	1	1
	V	1	1	2
	VI	1	1	1
	VII	1	1	1
	VIII	1	1	1
3	I	-	4	1
	II	4	-	4
	III	1	4	-
	IV	1	4	1
	V	1	3	1
	VI	1	4	1
	VII	1	4	1
	VIII	1	3	1
4	I	-	2	1
	II	2	-	3
	III	1	3	-
	IV	3	1	4
	V	1	1	1
	VI	1	2	1
	VII	1	2	1
	VIII	1	2	1

shown in the example of bruxism [26], but do not allow for the discovery and study of new patterns in data beyond previous knowledge. It should also be noted that dealing with multidimensional non-linear data is one of the challenges in the analysis of biomedical signals [49]. Visualisation of multivariate data in two-dimensions enables further interpretation of the results. Thus, not only information about the similarity between the entries is obtained, but also information about the entry itself (grouping samples of one entry into a small or large number of neurons).

Although the authors have endeavoured to comply with the standards listed in the testing guidelines for EMG provided by [39,50], the following limitations of the presented study should be taken into account.

- A commercial Noraxon system with a commercial Myoresearch software was used to collect and process the sEMG data and not every detail of the signal processing provided by the system is disclosed in the documentation. Although, recent study by [39] suggests that manufacturers should report the input impedance at 50 Hz or the input resistance and the input capacitance that is in parallel with it, Noraxon does not provide this information. Also, there is no detailed description of the implemented numerical algorithm to perform DC offset and zero offset correction available.
- It should be noted that this study does not include all muscles that act on the TMJ and are involved in the jaw movements considered in this study, e.g., the lateral and medial pterygoid muscles, which may be considered as a limitation of this study. We included only activation of superficial muscles that can be non-invasively tested under clinical conditions. Thanks to this approach, the methodology can be used widely in clinical practice to improve the diagnostic process.
- Moreover, the fat layer located above the belly of each tested muscle was not measured. However, the clinicians palpated the fat layers on each tested muscle and determined their thickness to be in the low range. Although, fat tissue attenuates sEMG signal, the normalisation of amplitude with respect to the MVC mitigates the problem of amplitude. This allowed us to match two signals using cross-correlation and compare all signals by applying SOM. In our study, the shape of processed sEMG plots (RMS envelopes) is especially important from the point of view of the performed analyses and discussion.
- One can argue that the electrode location on the muscle belly is not the best choice. Castroflorio et al. (2005) [51] suggests some optimal electrode location on masseter and temporalis for other type of electrodes (of a different shape and size). The influence of the electrode location used in our study on the results could be investigated in the future.
- As shown in literature [52], there are better procedures for skin treatment before sEMG testing than cleaning the skin with alcohol. However, clinicians pay attention that face skin is very subtle and cannot be damaged during the skin preparation.
- Next limitation is the low number of healthy patients. However, future studies may be supplemented by acquiring a larger number of datasets from both healthy patients and those patients with diagnosed TMD. Although, to identify a particular TMD, the activation pattern associated with that TMD would be required. Furthermore, testing a larger group of patients of both sexes would enable a discussion of this aspect as a factor.

5. Conclusions

The study is a step towards the classification of patients in terms of TMJ muscle activation using SOM. Together with the cross-correlation approach, SOM was used to interpret processed sEMG data obtained during the opening, closing, protrusion, and retrusion motions of the jaw. With reference to the postulated hypothesis, one can conclude:

1) With the ability to simultaneously consider four muscle activations, SOM may be used to classify patients in terms of jaw muscle activation (RMS pattern of sEMG).
2) Intra CC coefficients can be used to identify TMJ instability by assessing the similarity in muscle activation (RMS envelopes) in pairs of muscles (masseter, temporalis, ipsilateral and contralateral muscle pairs) in each tested time interval. This could be used in the planning of rehabilitation programmes.

The main novel aspects of the presented study are as follows:

1) TMJ issues are addressed by focusing on similarities in muscle activation at various levels with the use of CC and SOM.
2) An efficient approach toward a new classification has been proposed that does not depend on classic skeletal classes. The study shows how people can be grouped in terms of TMJ muscle activation.
3) SOM was applied to project and represent muscle activation during real jaw motions in various phases. This approach allows for the extraction of data similarities and dissimilarities between different subjects. Furthermore, at the same time, information is also obtained about a single subject.
4) The presented results provide more information on the activations of the masseter and temporalis in healthy humans during the opening, closing, protrusion, and retrusion of the jaw.

SOM analysis can be used further as a method for comparing individual responses, which, thanks to the possibility of clustering and large database access, could provide a classification of TMJ performance. It can provide a straightforward starting point for the diagnosis of similar dysfunctions, which is much needed for orthodontic and orthognathic treatment. The presented results support the stated hypotheses, although their verification in clinical conditions with a larger number of patients is still needed.

The analysis highlights the complexity of the stomatognathic system. Although the results show that muscle activity varies from person to person, the presented approach identifies similarities between individuals. The applied methods provide the basis for further studies into TMJ dysfunction, taking into account muscle activity and the dominant side. Future research should focus on determining the effects of connective tissue laxity and bruxism on the function of the temporomandibular joint.

To conclude, the SOM method enables comparison of neuromuscular responses by representing multidimensional data inputs. This can be useful in both biomechanical analysis and clinical practice. The presented approach can be used to create preventive models to identify dysfunction by analysing muscle activity and capturing jaw motion. In addition, SOM groups can be used to personalise predictive mathematical models of the stomatognathic system needed in the planning of orthognathic treatment. Moreover, this analysis can be performed under clinical conditions to assess muscle activity during treatment (e.g., using a tooth brace) and help decide whether corrections need to be made. It is worth noting that the SOM analysis is relatively user-friendly compared to the cross-correlation analysis of sEMG data, which requires greater experience. Especially valuable is the fact that SOM can analyse several muscle activations simultaneously. Therefore, it could be used to develop an efficient tool for daily clinical practice without complicating the diagnostic process. Future development should focus on gathering larger sets of data from various subjects for the automated classification of possible health problems.

CRediT authorship contribution statement

Mateusz Troka: Methodology, Software, Formal analysis, Writing – original draft, Writing – review & editing. **Wiktoria Wojnicz:** Conceptualization, Methodology, Investigation, Formal analysis, Writing – original draft, Writing – review & editing. **Katarzyna Szepietowska:** Validation, Formal analysis, Investigation, Writing – original draft, Writing – review & editing. **Marek Podlasiński:** Investigation. **Sebastian Walerzak:** Investigation. **Konrad Walerzak:** Investigation, Resources. **Izabela Lubowiecka:** Conceptualization, Supervision, Funding acquisition, Writing – original draft, Writing – review & editing.

Declaration of Competing Interest

The authors declare that they have no known competing financial interests or personal relationships that could have appeared to influence the work reported in this paper.

Acknowledgment

We would like to thank Prof. A. Tomaszewska and Mr P. Bielski for their help in data acquisition. Both are with the Gdansk University of Technology.

This study has been performed as part of the 3D-JAW Project (The study of 3D temporo-mandibular joint (TMJ) model of bone-cartilage-ligament system mapping for effective commercialization of results in dental prosthetics, orthodontic and orthognathic surgery; POIR.04.01.02-00-0029/17). The calculations were carried out at the Academic Computer Centre in Gdańsk (TASK), Poland.

Appendix A. Supplementary data

Supplementary data to this article can be found online at https://doi.org/10.1016/j.bspc.2021.103322.

References

[1] J. Bianchi, A.C. de Oliveira Ruellas, J.R. Gonçalves, B. Paniagua, J.C. Prieto, M. Styner, T. Li, H. Zhu, J. Sugai, W. Giannobile, E. Benavides, F. Soki, M. Yatabe, L. Ashman, D. Walker, R. Soroushmehr, K. Najarian, L.H.S. Cevidanes, Osteoarthritis of the Temporomandibular Joint can be diagnosed earlier using biomarkers and machine learning, Sci. Rep. 10 (2020) 1–14, https://doi.org/10.1038/s41598-020-64942-0.

[2] G. Tanteri, E. Tanteri, C. Tanteri, G. Slavicek. TMJ Dynamics, in: MRI Temporomandibular Jt, Springer International Publishing, Cham, 2020, pp. 57–90, https://doi.org/10.1007/978-3-030-25421-6_4.

[3] H.R. Mujakperuo, M. Watson, R. Morrison, T.V. Macfarlane, Pharmacological interventions for pain in patients with temporomandibular disorders, Cochrane Database Syst. Rev. (2010), https://doi.org/10.1002/14651858.cd004715.pub2.

[4] G. Dimitroulis, Temporomandibular disorders: a clinical update, Br. Med. J. 317 (7152) (1998) 190–194, https://doi.org/10.1136/bmj.317.7152.190.

[5] H.H. Tüz, Ç. Karaca, C. Özcan, Effect of suprahyoid muscles on mouth opening with and without lateral pterygoid muscle: 3D inverse dynamic model analysis, CRANIO® (2020) 1–10, https://doi.org/10.1080/08869634.2020.1745498.

[6] W. Wojnicz, I. Lubowiecka, A. Tomaszewska, K. Szepietowska, P. Bielski, Jaw biomechanics: Estimation of activity of muscles acting at the temporomandibular joint, AIP Conf. Proc. 2078 (2019), https://doi.org/10.1063/1.5092108.

[7] N.T. Artuğ, I. Goker, B. Bolat, O. Osman, E.K. Orhan, M.B. Baslo, New features for scanned bioelectrical activity of motor unit in health and disease, Biomed. Signal Process Control. 41 (2018) 109–128, https://doi.org/10.1016/j.bspc.2017.11.011.

[8] G.M. Tartaglia, G. Lodetti, G. Paiva, C.M.D. Felicio, C. Sforza, Surface electromyographic assessment of patients with long lasting temporomandibular joint disorder pain, J. Electromyogr. Kinesiol. 21 (4) (2011) 659–664, https://doi.org/10.1016/j.jelekin.2011.03.003.

[9] J.C. Pinho, F.M. Caldas, M.J. Mora, U. Santana-PenIn, Electromyographic activity in patients with temporomandibular disorders, J. Oral Rehabil. 27 (11) (2000) 985–990, https://doi.org/10.1111/j.1365-2842.2000.00571.x.

[10] L. Szyszka-Sommerfeld, M. Machoy, M. Lipski, K. Woźniak, The diagnostic value of electromyography in identifying patients with pain-related temporomandibular disorders, Front. Neurol. 10 (2019) 1–7, https://doi.org/10.3389/fneur.2019.00180.

[11] M.A.Q. Al-Saleh, C. Flores-Mir, N.M.R. Thie, Electromyography in diagnosing temporomandibular disorders, J. Am. Dent. Assoc. 143 (2012) 351–362, https://doi.org/10.14219/jada.archive.2012.0177.

[12] U. Santana-Mora, M. López-Ratón, M.J. Mora, C. Cadarso-Suárez, J. López-Cedrún, U. Santana-Penín, Surface raw electromyography has a moderate discriminatory capacity for differentiating between healthy individuals and those with TMD: a diagnostic study, J. Electromyogr. Kinesiol. 24 (3) (2014) 332–340, https://doi.org/10.1016/j.jelekin.2014.03.001.

[13] R. Latif, S. Sanei, C. Shave, E. Carter, Classification of Temporomandibular disorder from electromyography signals via Directed Transfer Function, Proc. 30th Annu. Int. Conf. IEEE Eng. Med. Biol. Soc. EMBS'08 - "Personalized Healthc. through Technol. 2 (2008) 2904–2907, https://doi.org/10.1109/IEMBS.2008.4649810.

[14] M. Ghodsi, H. Hassani, S. Sanei, Y. Hicks, The use of noise information for detection of temporomandibular disorder, Biomed. Signal Process Control. 4 (2) (2009) 79–85, https://doi.org/10.1016/j.bspc.2008.10.001.

[15] L.A. García-Espinosa, A. Minor-Martínez, F. Pérez-Escamirosa, J. Morales-González, I. Rodríguez-Castañeda, B. Flores-Ramírez, N. Pacheco-Guerrero, F. Ángeles-Medina, Multi-fractal DFA analysis of masseter muscles SEMG signal in patients with TMD, pilot study, Biomed. Signal Process. Control. 68 (2021), 102732, https://doi.org/10.1016/j.bspc.2021.102732.

[16] T.A.L. Wren, K. Patrick Do, S.A. Rethlefsen, B. Healy, Cross-correlation as a method for comparing dynamic electromyography signals during gait, J. Biomech. 39 (14) (2006) 2714–2718, https://doi.org/10.1016/j.jbiomech.2005.09.006.

[17] C.A. Moore, A. Smith, R.L. Ringel, Task-specific organization of activity in human jaw muscles, J. Speech, Lang Hear. Res. 31 (4) (1988) 670–680, https://doi.org/10.1044/jshr.3104.670.

[18] M. Garofalo, T. Nieus, P. Massobrio, S. Martinoia, Evaluation of the performance of information theory-based methods and cross-correlation to estimate the functional connectivity in cortical networks, PLoS ONE 4 (8) (2009) e6482, https://doi.org/10.1371/journal.pone.0006482.

[19] J. Yousefi, A. Hamilton-Wright, Characterizing EMG data using machine-learning tools, Comput. Biol. Med. 51 (2014) 1–13, https://doi.org/10.1016/j.compbiomed.2014.04.018.

[20] E. Gokgoz, A. Subasi, Comparison of decision tree algorithms for EMG signal classification using DWT, Biomed. Signal Process, Control. 18 (2015) 138–144, https://doi.org/10.1016/j.bspc.2014.12.005.

[21] M.-F. Lucas, A. Gaufriau, S. Pascual, C. Doncarli, D. Farina, Multi-channel surface EMG classification using support vector machines and signal-based wavelet optimization, Biomed. Signal Process Control. 3 (2) (2008) 169–174, https://doi.org/10.1016/j.bspc.2007.09.002.

[22] A. Nishad, A. Upadhyay, R.B. Pachori, U.R. Acharya, Automated classification of hand movements using tunable-Q wavelet transform based filter-bank with surface electromyogram signals, Futur. Gener. Comput. Syst. 93 (2019) 96–110, https://doi.org/10.1016/j.future.2018.10.005.

[23] A. Nishad, A. Upadhyay, G. Ravi Shankar Reddy, V. Bajaj, Classification of epileptic EEG signals using sparse spectrum based empirical wavelet transform, Electron. Lett. 56 (25) (2020) 1370–1372, https://doi.org/10.1049/el.2020.2526.

[24] K.S. Lee, H.J. Kwak, J.M. Oh, N. Jha, Y.J. Kim, W. Kim, U.B. Baik, J.J. Ryu, Automated detection of TMJ osteoarthritis based on artificial intelligence, J. Dent. Res. 99 (12) (2020) 1363–1367, https://doi.org/10.1177/0022034520936950.

[25] H. Kalani, S. Moghimi, A. Akbarzadeh, SEMG-based prediction of masticatory kinematics in rhythmic clenching movements, Biomed. Signal Process Control. 20 (2015) 24–34, https://doi.org/10.1016/j.bspc.2015.04.003.

[26] T. Sonmezocak, S. Kurt, Machine learning and regression analysis for diagnosis of bruxism by using EMG signals of jaw muscles, Biomed. Signal Process. Control. 69 (2021), 102905, https://doi.org/10.1016/j.bspc.2021.102905.
[27] T. Kohonen. Self-Organizing Maps, Springer, 1997, https://doi.org/10.1007/978-3-642-97966-8.
[28] A. Ijaz, J. Choi, Anomaly detection of electromyographic signals, IEEE Trans. Neural Syst. Rehabil. Eng. 26 (4) (2018) 770–779, https://doi.org/10.1109/TNSRE.2018.2813421.
[29] M. Milosevic, K.M. Valter McConville, E. Sejdic, K. Masani, M.J. Kyan, M. R. Popovic, Visualization of trunk muscle synergies during sitting perturbations using Self-Organizing Maps (SOM), IEEE Trans. Biomed. Eng. 59 (9) (2012) 2516–2523, https://doi.org/10.1109/TBME.2012.2205577.
[30] Z. Lv, F. Xiao, Z. Wu, Z. Liu, Y. Wang, Hand gestures recognition from surface electromyogram signal based on self-organizing mapping and radial basis function network, Biomed. Signal Process. Control. 68 (2021), 102629, https://doi.org/10.1016/j.bspc.2021.102629.
[31] M.H. Jali, Z.H. Bohari, M.F. Sulaima, M.N.M. Nasir, H.I. Jaafar, Classification of EMG signal based on human percentile using SOM, Res. J. Appl. Sci. Eng. Technol. 8 (2014) 235–242. 10.19026/rjaset.8.965.
[32] F. Mongini, M. Italiano, TMJ disorders and myogenic facial pain: a discriminative analysis using the McGill Pain Questionnaire, Pain 91 (2001) 323–330, https://doi.org/10.1016/S0304-3959(00)00461-9.
[33] M. Troka, W. Wojnicz, K. Szepietowska, I. Lubowiecka, Self-Organising map neural network in the analysis of electromyography data of muscles acting at temporomandibular joint, in: F. Chinesta, R. Abgrall, O. Allix, D. Néron, M. Kaliske (Eds.) 14th World Congress in Computational Mechanics, WCCM 2020,11-15 January 2021, Paris, France, CIMNE (2021), pp. 1445, https://www.wccm-eccomas2020.org/frontal/docs/WCCM-XIV-ECCOMAS-2020.pdf.
[34] A.H. Alghadir, H. Zafar, Z. Iqbal, A.,Effect of three different jaw positions on postural stability during standing, Funct. Neurol. 30 (2015) 53, https://doi.org/10.11138/FNeur/2015.30.1.053.
[35] C. Turkmen, G. Harput, G.I. Kinikli, N. Kose, H. Guney Deniz, Correlation of force sense error test measured by a pressure biofeedback unit and EMG activity of quadriceps femoris in healthy individuals, J. Electromyogr. Kinesiol. 49 (2019) 102366, https://doi.org/10.1016/j.jelekin.2019.102366.
[36] J. Knox, A. Gupta, H.A. Banwell, L. Matricciani, D. Turner, Comparison of EMG signal of the flexor hallucis longus recorded using surface and intramuscular electrodes during walking, J. Electromyogr. Kinesiol. 60 (2021), 102574, https://doi.org/10.1016/j.jelekin.2021.102574.
[37] B. Niespodziński, J. Mieszkowski, M. Kochanowicz, A. Kochanowicz, J. Antosiewicz, Effect of 10 consecutive days of remote ischemic preconditioning on local neuromuscular performance, J. Electromyogr. Kinesiol. 60 (2021), https://doi.org/10.1016/j.jelekin.2021.102584.
[38] G. Rasool, N. Bouaynaya, K. Iqbal, G. White, Surface myoelectric signal classification using the AR-GARCH model, Biomed. Signal Process, Control. 13 (2014) 327–336, https://doi.org/10.1016/j.bspc.2014.06.001.
[39] R. Merletti, G.L. Cerone, Tutorial. Surface EMG detection, conditioning and pre-processing: Best practices, J. Electromyogr. Kinesiol. 54 (2020) 102440, https://doi.org/10.1016/j.jelekin.2020.102440.
[40] T. Ishii, N. Narita, H. Endo, Evaluation of jaw and neck muscle activities while chewing using EMG-EMG transfer function and EMG-EMG coherence function analyses in healthy subjects, Physiol. Behav. 160 (2016) 35–42, https://doi.org/10.1016/j.physbeh.2016.03.023.
[41] A. Falaki, X. Huang, M.M. Lewis, M.L. Latash, Impaired synergic control of posture in Parkinson's patients without postural instability, Gait Posture. 44 (2016) 209–215, https://doi.org/10.1016/j.gaitpost.2015.12.035.
[42] Athanasios Papoulis; S Unnikrishna Pillai, Probability, Random Variables, and Stochastic Processes, McGraw-Hill, Boston, 2002.
[43] T.R. Derrick, J.M. Thomas, Time-series analysis: the cross-correlation function, Innov. Anal. Hum. Mov. (2004) 189–205.
[44] P. Marshall, B. Murphy, The validity and reliability of surface EMG to assess the neuromuscular response of the abdominal muscles to rapid limb movement, J. Electromyogr. Kinesiol. 13 (5) (2003) 477–489, https://doi.org/10.1016/S1050-6411(03)00027-0.
[45] T. Kohonen, MATLAB implementations and applications of the Self- Organising Map, 2014. http://docs.unigrafia.fi/publications/kohonen_teuvo/MATLAB_implementations_and_applications_of_the_self_organizing_map.pdf.
[46] H. Yin, The self-organizing maps: background, theories, extensions and applications, Stud. Comput. Intell. 115 (2008) 715–762, https://doi.org/10.1007/978-3-540-78293-3_17.
[47] J. Lötsch, A. Ultsch, Exploiting the Structures of the U-Matrix, in: Adv. Intell. Syst. Comput, Springer Verlag, 2014, pp. 249–257, https://doi.org/10.1007/978-3-319-07695-9_24.
[48] H.J. Vesanto, Juha, SOM Toolbox for Matlab 5, 2 (2000).
[49] S. Krishnan, Y. Athavale, Trends in biomedical signal feature extraction, Biomed. Signal Process Control. 43 (2018) 41–63, https://doi.org/10.1016/j.bspc.2018.02.008.
[50] M. Besomi, P.W. Hodges, J. Van Dieën, R.G. Carson, E.A. Clancy, C. Disselhorst-Klug, A. Holobar, F. Hug, M.C. Kiernan, M. Lowery, K. McGill, R. Merletti, E. Perreault, K. Søgaard, K. Tucker, T. Besier, R. Enoka, D. Falla, D. Farina, S. Gandevia, J.C. Rothwell, B. Vicenzino, T. Wrigley, Consensus for experimental design in electromyography (CEDE) project: electrode selection matrix, J. Electromyogr. Kinesiol. 48 (2019) 128–144, https://doi.org/10.1016/j.jelekin.2019.07.008.
[51] T. Castroflorio, D. Farina, A. Bottin, M.G. Piancino, P. Bracco, R. Merletti, Surface EMG of jaw elevator muscles: effect of electrode location and inter-electrode distance, J. Oral Rehabil. 32 (6) (2005) 411–417, https://doi.org/10.1111/j.1365-2842.2005.01442.x.
[52] G. Piervirgili, F. Petracca, R. Merletti, A new method to assess skin treatments for lowering the impedance and noise of individual gelled Ag-AgCl electrodes, Physiol. Meas. 35 (10) (2014) 2101–2118, https://doi.org/10.1088/0967-3334/35/10/2101.